Nonlinear Dynamics of Magnetic Islands Imbedded in Small-Scale Turbulence

M. Muraglia,[1] O. Agullo,[1] S. Benkadda,[1] X. Garbet,[2] P. Beyer,[1] and A. Sen[3]
[1]France-Japan Magnetic Fusion Laboratory, LIA 336 CNRS, Marseille, France
[2]CEA, IRFM, 13108, St-Paul-Lez-Durance, France
[3]Institute for Plasma Research, Bhat, Gandhinagar 382428, India
(Received 2 September 2008; published 29 September 2009)

The nonlinear dynamics of magnetic tearing islands imbedded in a pressure gradient driven turbulence is investigated numerically in a reduced magnetohydrodynamic model. The study reveals regimes where the linear and nonlinear phases of the tearing instability are controlled by the properties of the pressure gradient. In these regimes, the interplay between the pressure and the magnetic flux determines the dynamics of the saturated state. A secondary instability can occur and strongly modify the magnetic island dynamics by triggering a poloidal rotation. It is shown that the complex nonlinear interaction between the islands and turbulence is nonlocal and involves small scales.

DOI: 10.1103/PhysRevLett.103.145001 PACS numbers: 52.35.Ra, 52.55.Fa, 52.55.Tn

Magnetic reconnection is a complex phenomenon involving plasma flows and a rearrangement of the magnetic field lines inside a narrow region (the reconnection layer) where topologically different magnetic flux tubes can get interconnected and reconfigure themselves. It plays an important role in fusion experiments as well as in many astrophysical events [1]. In a complex fusion device, such as a tokamak, the plasma is susceptible to many kinds of instabilities which can occur concurrently at various space and time scales. Such a coexistence of microturbulence and magnetohydrodynamic activities has been observed in many experiments [2] with some evidence of correlated effects arising from their simultaneous existence. An important question to address is therefore the nature and amount of mutual interaction between microturbulence and large-scale MHD instabilities—an issue that is at the heart of multiscale phenomena of complex systems in astrophysics, geophysics, nonlinear dynamics, and fluid turbulence. Early analytic attempts at investigation of this important question have relied on *ad hoc* modeling of turbulence effects through anomalous transport coefficients [3]. More recently a minimal self-consistent model based on wave kinetics and adiabatic theory has been used in [4] to study the interaction of a tearing mode with drift wave turbulence. Numerical simulation studies in [5] have directly addressed the problem of multiscale interactions and have taken into account the nonlinear modifications of the equilibrium profiles due to turbulence. Such studies have been extended in [6] to investigate the interaction between double tearing modes and microturbulence through the excitation of zonal flows. Finally in [7] a numerical investigation of the interaction of a 2D electrostatic turbulence with an island whose dynamics is not fully self-consistent but is governed by a generalized Rutherford equation has been carried out. In this Letter we report on self-consistent simulations of the multiscale interaction between microturbulence driven by pressure gradients and magnetic islands with a focus on regimes where the growth of the latter is essentially due to pressure effects and where small-scale dynamics appear to be important. The background microturbulence is found to induce a nonlinear rotation of the island as well as to significantly alter its final quasiequilibrium state by the excitation of a secondary instability. We discuss the characteristics of the various stages of the nonlinear evolution and also delineate the role of small scales in the overall dynamics of the system.

We consider a minimalist two-dimensional plasma model based on the two fluid Braginskii equations in the drift approximation [8,9] with cold ions and isothermal electrons. The model includes magnetic curvature effects and electronic diamagnetic effects but neglects electron inertia and Hall effect contributions. The evolution equations are

$$\frac{\partial}{\partial t}\nabla_\perp^2\phi + [\phi, \nabla_\perp^2\phi] = [\psi, \nabla_\perp^2\psi] - \kappa_1\frac{\partial p}{\partial y} + \mu\nabla_\perp^4\phi, \quad (1)$$

$$\frac{\partial}{\partial t}p + [\phi, p] = -v_\star\left((1-\kappa_2)\frac{\partial\phi}{\partial y} + \kappa_2\frac{\partial p}{\partial y}\right) + \hat{\rho}^2[\psi, \nabla_\perp^2\psi] + \chi_\perp\nabla_\perp^2 p, \quad (2)$$

$$\frac{\partial}{\partial t}\psi = [\psi, \phi - p] - v_\star\frac{\partial\psi}{\partial y} + \eta\nabla_\perp^2\psi, \quad (3)$$

where the dynamical field quantities are the electrostatic potential ϕ, the electron pressure p, and the magnetic flux ψ. The equilibrium quantities are a constant pressure gradient and a magnetic field corresponding to a Harris current sheet model [1]. Further, $\kappa_1 = 2\Omega_i\tau_A\frac{L_\perp}{R_0}$ and $\kappa_2 = \frac{10}{3}\frac{L_p}{R_0}$ are the curvature terms with R_0 representing the major radius of a toroidal plasma configuration. L_p is the gradient scale length, τ_A is the Alfvén time based on a reference perpendicular length scale $L_\perp$, and Ω_i is the ion cyclotron frequency. Equations (1)–(3) are normalized using the characteristic Alfvén speed v_A and the length scale $L_\perp$.

μ is the viscosity, $\chi_\perp$ is the perpendicular diffusivity, η is the plasma resistivity, $v_\star = \beta_e/\Omega_i\tau_A$ is the normalized electron diamagnetic drift velocity with β_e being the ratio between the electronic kinetic pressure and the magnetic pressure. $\hat{\rho} = \frac{\rho_s}{L_\perp}$ is the normalized ion sound Larmor radius. In the limit $R_0 \to 0$, we recover the drift tearing model [9], and when magnetic fluctuations are weak, $\psi \sim 0$ ($\kappa_1 \neq 0$), the system describes the electrostatic interchange instability. Conversely, the large island limit, $\hat{\rho} = v_\star = 0$ with $\Omega_i\tau_A \sim 1$, gives the high β model which was originally introduced by Strauss [10]. The minimalist model used here is, in fact, a reduced version of the four fields model derived in Ref. [11] where we have ignored the parallel ion dynamics and thereby neglected its effect on the transversal pressure balance [11].

As a preliminary to the numerical study of Eqs. (1)–(3), we first look at some linear results of a simplified set of equations with $\mu = \chi_\perp = \kappa_i = 0$ where it is possible to obtain analytic relations for the linear growth rate of the tearing mode under the constant ψ approximation [1,12], namely,

$$\Delta' = \frac{\gamma^2}{k_y^2}\alpha^{-3}\int_{-\infty}^{+\infty}\frac{\chi''(z)}{z}dz, \qquad z = -z^2\chi(z) + (1+\hat{\rho}^2\alpha^{-2}z^2)\chi''(z), \tag{4}$$

where $\phi(x) = -\alpha^{-1}\psi(0)\chi(z)$, $z = \alpha x$, $\alpha = (\eta\gamma/k_y^2)^{1/4}$, and Δ' is the standard stability parameter. The perturbed pressure is given by $p(x) = \hat{\rho}^2\phi''(x)$ (with $\hat{\rho} = 0$ corresponding to the classical tearing situation). Figure 1 shows the dependence of the linear growth rate $\gamma(\eta)$ of the instability on the resistivity with $\hat{\rho} = 10^{-1}$. The numerical results (circles) are seen to agree quite well with the values (diamonds) of the solution to the analytic relation Eq. (4). We observe that $\gamma(\eta)$ exhibits a change of slope after a certain value of η. The two regimes correspond to the two limiting cases $T_e = 0$ or $p = 0$ (solid line) and $\phi = 0$ (dash-dotted line). The intersection of the two lines gives the critical value of the resistivity $\eta_c = 0.58\Delta'^{-1/2}\hat{\rho}^{5/2} \sim 8\times10^{-4}$ for $\Delta' = 6$. When $\eta > \eta_c$, the linear growth rate given by the classical tearing case is higher than the other limiting case. The system chooses the more unstable case and the classical tearing mode is recovered with the scaling laws $\gamma \sim \eta^{3/5}$ and $\delta \sim \eta^{2/5}$. When $\eta < \eta_c$, the coupling between p and ψ is strong and the island formation is driven by the pressure perturbation. The resistive layer becomes thinner or more singular than in the case $T_e = 0$ where only a (ϕ, ψ) coupling exists. Further, the disagreement observed between the numerical and the theoretical results for $\eta > 5\times10^{-2}$ is a consequence of the breaking down of the constant ψ approximation in this regime.

We now discuss the full nonlinear numerical simulation of Eqs. (1)–(3) that explores the mutual interaction between small-scale interchange modes and a small magnetic island. A semispectral code with a 2/3 dealiasing rule in the poloidal direction, a resolution of 128 grid points in the radial direction, 96 poloidal modes, and that maintains

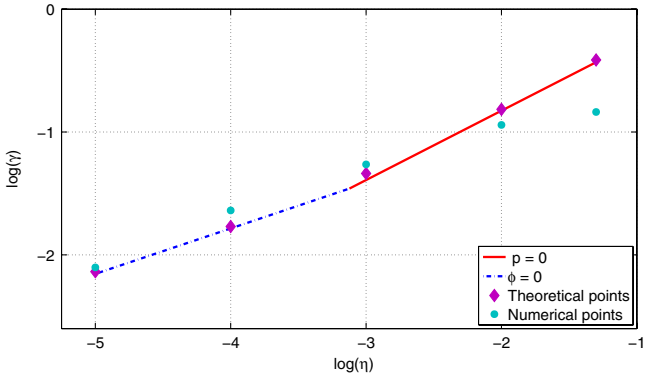

FIG. 1 (color online). Numerical and theoretical results of the linear growth rate γ vs η at $\nu = \chi_\perp = 0$, $\Delta' = 6$, and $\hat{\rho} = 10^{-1}$.

conservation properties of the nonlinear terms to a high degree has been used. The computational box size is $L_x = L_y = 2\pi$. In order to isolate the nonlinear mechanisms responsible for the island rotation, the linear diamagnetic effect has been turned off in Eq. (3). The effect of the latter on the evolution of the tearing mode is well known, namely, that it leads to a real frequency and consequently a rotation of the island in the diamagnetic drift direction. Note that we have checked *a posteriori* by turning on the linear diamagnetic term in Eq. (3) that the amount of induced nonlinear rotation (obtained by subtracting the linear diamagnetic frequency from the total rotation) remains the same. In Eq. (3) we also set $\kappa_2 = 0$, since we find from our simulations that the κ_2 contribution is rather weak. $\hat{\rho}$ and $v_\star$ are taken to be equal to 1 and $\beta_e = 10^{-2}$. The parameter related to the interchange instability is $\kappa_1 = 10^{-2}$. The shape of the equilibrium magnetic field is chosen to allow a tearing instability to develop with a poloidal mode number $k_y = 1$ with $\Delta' = 6$ [1]. Figure 2 shows, for $\mu = \chi_\perp = \eta = 10^{-4}$, the time evolution of the magnetic (E_ψ), pressure (E_p), and kinetic (E_ϕ) energies of the fluctuations for $\eta < \eta_c$, corresponding to a regime where the magnetic island generation is pressure driven. Four phases are observed. First, an exponential growth of the magnetic island ($t \lesssim 1300\tau_A$), followed by a quasiplateau phase with, however, an increase of the energies of the three fields ($t \lesssim 4500\tau_A$). Next, a phase characterized by an abrupt growth of the kinetic and pressure energies in which the kinetic energy level equals the energy of pressure perturbations, and finally, the system reaches a new quasiplateau phase for ($t \gtrsim 5100\tau_A$). During the linear and first plateau phases, the energy associated with the pressure perturbations is higher than the kinetic energy; i.e., the dynamics is controlled by an interplay between the magnetic flux and the pressure. In the second phase, $t \lesssim 4500\tau_A$, the magnetic island is maintained by adjacent pressure cells similar to what is usually observed for flow cells in the nonlinear regime of a tearing island [1]. This is illustrated in Fig. 3 (upper panel, $t = 3000\tau_A$). During this phase, the kinetic energy piles up in the flow cells which are located in the vicinity of the island. After $t \sim 3600\tau_A$,

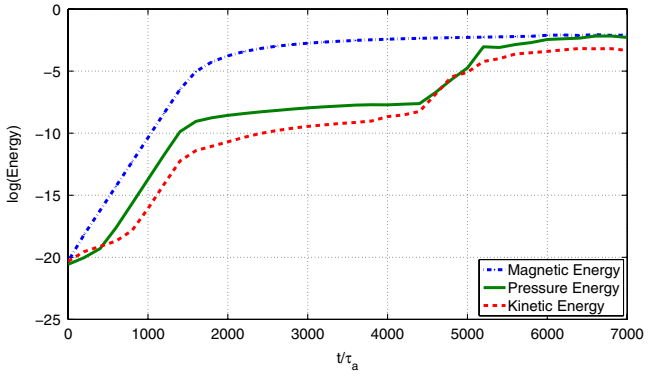

FIG. 2 (color online). Time evolution of the magnetic, pressure, and kinetic energies.

the flow cells are no longer located in the vicinity of the magnetic island. At $t \gtrsim 4500\tau_A$, a sharp growth of the kinetic and pressure energies occurs. Far from the island the current is not significant, and for $t/\tau_A \in [4500, 5000]$, a dominant interchange mode outside the sheet (ϕ_{11}, p_{11}) is enhanced. The associated kinetic and pressure energies of the latter are equal. Here, ϕ_{11} means $\phi(k_x = 1, k_y = 1)$. The competition between the interchange and tearing modes leads to the generation of small-scale pressure structures in the vicinity of the island that suffer further destabilization leading to a drastic modification of the dynamics. Indeed, in less than 200 Alfvén times, around $t \sim 5000\tau_A$, an abrupt growth of the energy contained in the pressure perturbation is observed and the system dynamics changes; i.e., a bifurcation occurs. At larger times, $t > 5100\tau_A$, the pressure dominates over the flow, $E_p \gg E_\phi$, and the size of the magnetic island finally saturates. Figure 4 shows the energy spectra of the fields just before and after the bifurcation. Before the bifurcation, the interchange mode is observed at $k_y = 1$, and as long as $k_y \geq 2$, the pressure energy is much higher than the kinetic energy. After this dynamical bifurcation, we observe a persistence of small scales as well as an enhancement of the energies [Fig. 4(b)]. We also find that a mean poloidal pressure and flow have been generated, and as we will see below, it is linked to the rotation properties of the island. For $8 \leq k_y \leq 50$, there is a trend towards an equipartition of the magnetic and pressure spectra. It is worth noting that even though the magnetic island is still, at this point, in a quasilinear stage (the magnetic energy being concentrated on the mode $k_y = 1$), the pressure perturbation has a fully nonlinear structure and is made up mainly of the modes $k_y < 7$. An interesting feature clearly observed in the snapshot shown in Fig. 3 at $t = 6000\tau_A$ is the generation of an island structure in the pressure field containing almost 90% of the pressure energy E_p.

In the final stage where the energies reach a new quasiplateau, as observed in Fig. 2, the change of dynamics is characterized by two important macroscopic features. First, there is a change of symmetry—the poloidal diamagnetic velocity $v_{\rm dia} = \frac{\partial}{\partial x}\langle p \rangle_y$ having even parity for $t \lesssim 5100\tau_A$ (brackets mean an average over the poloidal direction) loses this property after the bifurcation and has in fact an odd parity in the vicinity of the current sheet. This change of parity is clearly shown in Fig. 5 where $v_{\rm dia}$ is plotted, before and after the transition, at $t = 3000\tau_A$ and $t = 6000\tau_A$, respectively. The second macroscopic change is the inversion of the poloidal rotation direction of the magnetic island together with an amplification of the velocity. The amplified velocity arising from the nonlinear interactions is of the order of the linear diamagnetic velocity as verified from *a posteriori* runs made with the linear diamagnetic term retained in the equations. The change of direction in the island rotation can be observed in the zoomed frame of Fig. 6 which shows the time evolution of the poloidal position of the island. We find that the increase of $v_{\rm dia}$ at the transition is linked to the coincident growth of the interchange mode (ϕ_{11}, p_{11}) which feeds the angular momentum. The detailed mecha-

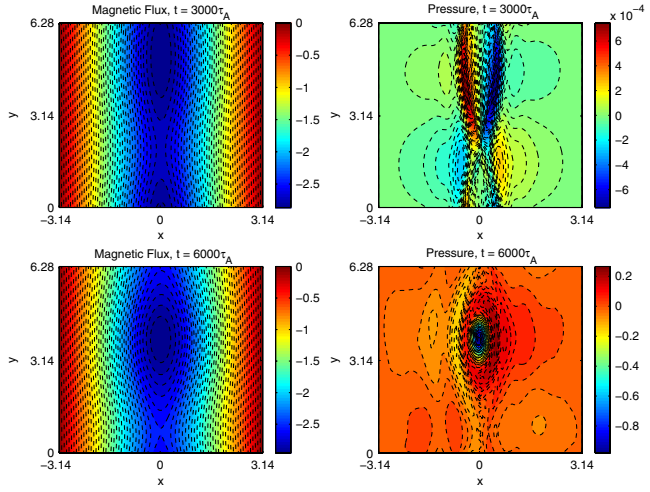

FIG. 3 (color online). Snapshots of the magnetic flux and the pressure at $t = 3000\tau_A$ (upper panel) and $t = 6000\tau_A$ (lower panel).

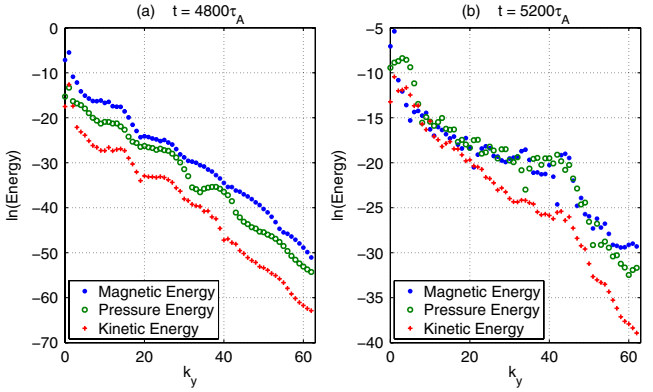

FIG. 4 (color online). Spectral energy densities as functions of the poloidal mode number k_y, just (a) before (at $t = 4800\tau_A$) and (b) after (at $t = 5200\tau_A$) the bifurcation.

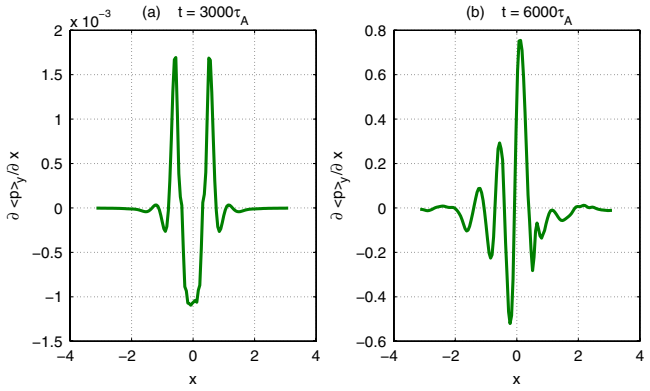

FIG. 5 (color online). Plots of the poloidal diamagnetic velocity $v_{\rm dia}$ at $t = 3000\tau_A$ (a) and $t = 6000\tau_A$ (b).

nism of this nonlinear generation of angular momentum is, however, not known at this time and remains an open question.

Some insights into the origin of the island poloidal rotation can be obtained from Eq. (3) where one notes that both the self-generated zonal and diamagnetic flow terms, $v_{\rm zon} = \frac{\partial}{\partial x}\langle\phi\rangle_y$ and $v_{\rm dia}$, can produce a poloidal rotation of the island. To investigate the role of these flows, we have plotted in Fig. 6 the poloidal position of the center of the island $y_{\rm island}$ and the poloidal positions related to the contributions of the diamagnetic velocity $v_{\rm dia}$ and the zonal flow velocity $v_{\rm zon}$. More precisely, we have plotted $y_{\rm dia}(t) = (1/\delta)\int_0^t dt \int_{-\delta/2}^{\delta/2} dx v_{\rm dia}(x,t)$ and $y_{p,\phi} = (1/\delta)\times \int_0^t dt \int_{-\delta/2}^{\delta/2} dx (v_{\rm dia} - v_{\rm zon})$. We observe that the model $y_{\rm dia}$ reproduces well the time evolution of the rotation of the island, before and after the bifurcation. At larger times, $t \gtrsim 6000\tau_A$, we observe that the contribution of the zonal flow cannot be neglected, even if the rotation of the island is mainly governed by the nonlinear generation of poloidal diamagnetic velocity. In [9], a similar approach was taken, without an averaging over the sheet, and a value of the velocity at the center of the sheath was used.

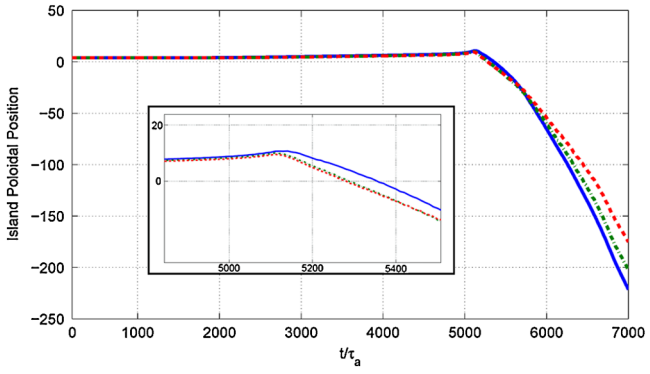

FIG. 6 (color online). Time evolution of the poloidal position of the center of the magnetic island $y_{\rm island}(t)$ (solid blue line) and the models $y_{\rm dia}(t)$ (dashed red line), $y_{p,\phi}(t)$ (dash-dotted green line).

To summarize, we have shown that the dynamics of magnetic islands can be strongly affected by the presence of a background of interchange modes. In the low resistivity and/or small Δ' limit, the coupling between the magnetic flux and the pressure is dominant compared to that between the magnetic flux and the plasma potential. In the asymptotic nonlinear regime, a pressure island structure builds up and the pressure pattern is not a flux function except in the center of the magnetic island. In fact, this regime is a result of a novel nonlinear transition that is observed for a wide range of parameters when the condition $\eta < \eta_c$ is satisfied. It is initiated by electrostatic interchange modes which compress the magnetic structure and generate small scales inside the island. Another noteworthy finding is that the bifurcation leads to a change of symmetry of the diamagnetic velocity that occurs when the energy of the large-scale interchange mode is of the same order of magnitude as the thermal energy contained in the cell maintaining the magnetic structure. The destabilization leads to a poloidal rotation of the island that is linked to the nonlinearly generated diamagnetic velocity in the current sheet. The basic phenomena highlighted by our results are reproducible over a large region of parametric space, and in that sense appear to be generic albeit within the constraints of our minimalist model. Effects ignored in our model including parallel heat conduction, parallel ion dynamics, and contributions of the Hall and electron inertia terms may bring about some modifications. Investigation of such effects in an enlarged model are therefore necessary to provide a more global perspective of this complex phenomena and for which our present studies provide a minimalist and basic description.

[1] D. Biskamp, *Magnetic Reconnection in Plasmas* (Cambridge University Press, Cambridge, England, 2000).
[2] K. Tanaka *et al.*, Nucl. Fusion **46**, 110 (2006); E. Joffrin *et al.*, Nucl. Fusion **43**, 1167 (2003).
[3] P. K. Kaw, E. J. Valeo, and P. H. Rutherford, Phys. Rev. Lett. **43**, 1398 (1979); A. K. Sundaram and A. Sen, Phys. Rev. Lett. **44**, 322 (1980); A. Furuya, S. Itoh, and M. Yagi, J. Phys. Soc. Jpn. **71**, 1261 (2002).
[4] C. J. McDevitt and P. H. Diamond, Phys. Plasmas **13**, 032302 (2006).
[5] A. Thyagaraja *et al.*, Phys. Plasmas **12**, 090907 (2005).
[6] A. Ishizawa and N. Nakajima, Nucl. Fusion **47**, 1540 (2007).
[7] F. Militello *et al.*, Phys. Plasmas **15**, 050701 (2008).
[8] B. D. Scott, J. F. Drake, and A. B. Hassam, Phys. Rev. Lett. **54**, 1027 (1985).
[9] M. Ottaviani, F. Porcelli, and D. Grasso, Phys. Rev. Lett. **93**, 075001 (2004).
[10] H. R. Strauss, Phys. Fluids **20**, 1354 (1977).
[11] R. D. Hazeltine, M. Kotschenreuther, and P. J. Morrison, Phys. Fluids **28**, 2466 (1985); R. D. Hazeltine and H. R. Strauss, Phys. Rev. Lett. **37**, 102 (1976).
[12] R. B. White, *The Theory of Toroidally Confined Plasmas* (Imperial College Press, London, 2001).